Journal of Photochemistry and Photobiology A: Chemistry 199 (2008) 14–22

Contents lists available at ScienceDirect

Journal of Photochemistry and Photobiology A: Chemistry

journal homepage: www.elsevier.com/locate/jphotochem

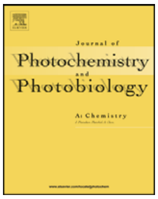

Major products in the photochemistry of perylene adsorbed in models of atmospheric particulate matter

Pura Sotero, Rafael Arce*

Department of Chemistry, University of Puerto Rico, Río Piedras Campus P.O. Box 23346, San Juan 00931-3346, Puerto Rico

ARTICLE INFO

Article history:
Received 26 October 2007
Received in revised form 5 April 2008
Accepted 20 April 2008
Available online 29 April 2008

Keywords:
PAH
Perylene
Photochemistry
Silica gel
Alumina

ABSTRACT

The photodegradation of adsorbed perylene is strongly influenced by the environment in which it is found as demonstrated by the nature of the photoproducts characterized on the adsorbed state in comparison to its photochemical behavior in solution. The separation, characterization, and identification of the products were carried out using HPLC equipped with UV–vis diode array and MS detection. Two of the products were identified as 1,12-perylenedione and 3,10-perylenedione. Three additional products were characterized as a perylenedione and two perylenediols based on their m/z ratio. Based on this information, two possible mechanisms of formation were proposed for the identified diones. The experimental data showed that both the radical cation and singlet oxygen participate in the route of photodegradation of perylene which occurs through a mixed Type I and Type II pathways. These results assist in the understanding of complex processes undergone by perylene and other PAHs in the environment.

1. Introduction

Perylene, Per, is a polycyclic aromatic hydrocarbon (PAH) found ubiquitously as an environmental contaminant. It has been identified in products of incomplete combustion such as cigarette smoke and engine exhaust, as well as smoked food products and in emissions of oil fires, fly ash from municipal waste incinerations, asphalt plants, and cooking plants. Per is also one of the few PAHs found in nature whose source can include soil, dust-rise by wind, sea spray, forest fires, volcanic dust, and some vegetation [1–8]. Most airborne hydrocarbons are associated with particulate matter [9]. Because of its low vapor pressure, Per exists solely in the particulate phase in the ambient atmosphere.

The persistence of PAHs associated with fine airborne particulate matter is important not only because in the atmosphere they may be transported over long distances, but also because they can undergo chemical reactions. These transformations can lead to their degradation or to transformations into products more toxic than the parent compound [10]. Recent studies link air pollutants released from motor vehicles and power plants to health effects and higher death rates [11]. Because of the risks arising from pollution to human health and to the ecological equilibria, studies of the fate of atmospheric pollution are of great importance. In these terms, studies of the photodegradation of PAHs adsorbed on surfaces are of relevance for our understanding of the fate of these compounds in the atmosphere.

Fly ash produced in electric power plants consists mostly of aluminum–silicon–oxygen compounds, mixed with smaller amounts of sodium, magnesium, potassium, calcium, and titanium [12]. This is called the aluminosilicate matrix. For this reason, silica gel of different pore diameter and alumina has been used as model surfaces in our laboratory, because they resemble the composition of fly ash in particular and the atmospheric particulate matter in general.

Photodegradation studies of Per and other PAHs have focussed on the effect of the surface's chemical and physical properties such as color, carbon content, surface area, particle porosity, and size and surface loading upon the rate of phototransformation [13–15]. Photolytic half-lives highly dependent on the physical and chemical nature of the substrate have been reported [14]. For Per adsorbed on silica or alumina substrates, half-lives of 4.7 and 1.7 h have been calculated under specific laboratory experimental conditions [14]. Recently, more comprehensive mechanistic photochemical studies of other PAHs have been reported [16–27].

McDow et al. [28] reported that PAHs adsorbed onto atmospheric aerosol particles from sources such as diesel soot and wood smoke are found in an organic layer (possibly liquid) around a carbon core. The composition and polarity of this organic layer depends on the emission source, and can influence the decay of the PAHs. For these reasons, it was of interest to compare the effect of surface interactions on the photochemical behavior of perylene with that in solution. By analogy, this could provide information

---

* Corresponding author.
E-mail address: rarce@uprr.pr (R. Arce).

1010-6030/$ – see front matter © 2008 Elsevier B.V. All rights reserved.
doi:10.1016/j.jphotochem.2008.04.011

on the photodegradation mechanisms of PAHs when adsorbed in inorganic oxides in ashes versus those in diesel soot or wood smoke particles.

This study reports on the photochemistry of Per adsorbed on the inactivated surfaces of silica gel and alumina, and in some nonpolar and polar solvents as models of atmospheric particulate matter. The objective was to study the effect of the nature of the adsorbent or the solvent, the average pore diameter, coadsorbed gases and water, and surface loading on (1) the photochemical reactions, (2) the participating excited states and reactive intermediates in the photochemical reactions [29], and (3) the nature and yield of the products. Under these controlled laboratory conditions we were able to obtain some understanding of the more complex environment of an atmospheric aerosol. Because photodegradation products can be more toxic than the parent compound, it is important to characterize them, and to establish their possible routes of formation in order to understand their ultimate environmental fate.

2. Experimental

2.1. Reagents

Perylene (Gold Label, 99%), Methylene blue (83% Dye content), and 2,5-dimethylfuran (99%+) were obtained from Aldrich Chemical Co., Inc. 3,10-perylenedione (99%) was obtained from Dr. Ehrenstorfer GmbH, Reference Materials for Residual Analysis, Germany. Alumina (Type F-20), Silica Gel (pore size 25 Å, 100–200 mesh; pore size 40 Å, 35–70 mesh; pore size 60 Å, 130–270 mesh; pore size 150 Å, 60–200 mesh) were obtained from Sigma Chemical Co. and used unactivated as models of the atmospheric particulate. The solvents hexane, methanol, acetone, and acetonitrile (OPTIMA grade) were obtained from Fisher Scientific.

2.2. Instrumentation

The methods and instrumentation used in the absorption and fluorescence measurements have been described elsewhere [29].

A C_{18} Jupiter Column, 250 mm × 5 μm × 4.6 mm (Phenomenex), was used for the chromatographic separations in conjunction with a Hewlett Packard 1100 HPLC with a diode array detector. For the separation, the gradient employed started at 50:50 acetonitrile/water increased to 100% acetonitrile after 14 min, and returned to 70:30 acetonitrile/water after 28 min. The system was returned to 50:50 acetonitrile/water for the next run. The sample size injected was 15 μL at a flow rate of 1.00 mL/min and at a pressure of 93 bars. Each sample was injected at least 3 times.

The MS analysis was made with a Quattro VG Organic Mass Spectrometer using the Atmospheric Pressure Chemical Ionization (APcI) method in the positive mode. Per and the products of photodecomposition ionized readily upon elution from the column. The mass spectrometer was coupled with an HPLC (Hewlett Packard 1100). The flow rate of the mobile phase was 1.00 mL/min.

2.3. Sample preparation [29]

For the singlet oxygen experiments, either methylene blue or 2,5-dimethylfuran (DMF) was used as $^1O_2$ sensitizer and $^1O_2$ quencher, respectively. The methylene blue was dissolved in 100 mL of methanol and the silica gel was added and stirred for 5 min using 0.0135 g of methylene blue for each 2 g of silica gel. The solvent was removed by rotoevaporation. After this step, this silica gel was mixed with 4 g of a sample of Per adsorbed on silica gel. The DMF was coadsorbed on a sample of Per adsorbed on silica gel by exposing the sample inside a small chamber to the vapor pressure of DMF at 25 °C for 1 h. Thus, is assumed that under these conditions the quantity of DMF adsorbed is larger than the initial number of moles of Per (10^{-8} mol).

The reproducibility of sample preparation and of the loading procedure was established from the initial fluorescence or diffuse reflectance intensities.

2.4. Sample irradiation

Samples were photolyzed using an Oriel Xe–Hg ozone free 1000 W UV lamp which was located at an end of an optical bench. A cylindrical water filter was used to absorb IR radiation. Cold water was circulated through the filter to minimize the heating of the sample and avoid thermal reactions on the irradiated surface. A Corning 4–70 band-pass filter was used to isolate the wavelength range of 320–580 nm. Five grams of sample were placed in a Pyrex rotatory cell that was located 48 cm from the lamp housing. This cell has indentations on its inner surface to disperse the powder sample inside the cell as it is rotated, thus providing homogeneous mixing and irradiation when rotated [14,30]. For the sensitization experiments with singlet oxygen, a Corning 2–59 filter was used to prevent the sample from receiving wavelengths under 610 nm. Wavelengths greater that 610 nm are absorbed mainly by methylene blue.

2.5. Sample extraction

The powdered sample is placed inside a flask to which 30 mL of acetone were added. After stirring for 15 min with a magnetic stirrer, the sample was filtered and washed again with acetone. This process was repeated 3 times and the extract was then preconcentrated. The extraction efficiency was determined by visually inspecting the color of the silica and by recording the diffuse reflectance and fluorescence spectra of the surface after the extraction. After the extraction procedure, no absorption or fluorescence emissions were observed from the extracted silica indicating a high extraction efficiency.

Extractions at room temperature and the subsequent HPLC analysis of the sample were done immediately after the irradiations to avoid possible thermal degradation of the products.

2.6. Product quantization and data analysis

The amount of 3,10-perylenedione produced was calculated by using the area of the chromatographic peaks and the response factor from the HPLC. The response factor was calculated using the following equation:

$$f_\varepsilon = A/C \tag{1}$$

where A refers to the integrated peak area of the photoproduct, f_ε is the response factor which includes all the conditions including the molar absorption coefficient of the compound, and C refers to the moles of compound injected to the HPLC. The value of f_ε was obtained from a calibration curve generated using solutions of known concentrations of the standard of 3,10-perylenedione in ethyl acetate. From the slope of the resulting curve of peak area as a function of concentration (M), a value of $f_\varepsilon = 3 \times 10^7\ \mathrm{M}^{-1}$ was obtained. The response factors for the other products were not determined due to the unavailability of the standards.

The percent of products formed by reaction of perylene with singlet oxygen and by the radical intermediate pathway were calculated from a comparison of the peak areas of the extracted products from samples irradiated in the presence of air, A_0, (presence of radical intermediate species and singlet oxygen) and in the absence of singlet oxygen, A_1, (sample containing coadsorbed

2,5-dimethylfuran). The equation used for the calculation was:

$$\left\{\frac{(A_0-A_1)}{A_0}\right\}\times 100 \tag{2}$$

In reporting photodegradation rates and rate constants, correlation coefficients were used as a measure of the closeness of the fitting of the data to a linear function.

3. Results and discussion

3.1. Spectral changes during the photochemistry of perylene adsorbed on silica gel and alumina surfaces and in polar and nonpolar solvents

The phototransformations of adsorbed Per were studied as a function of the chemical nature of the surface (silica gel versus alumina), the surface loading, and in the presence of coadsorbed species (Argon, O_2), changing these variables one at a time. In samples irradiated under an O_2 atmosphere the intensity of the perylene's emission band decreased as a function of irradiation time and a broad band with a maximum at 487 nm was formed (Fig. 1A). Also, new absorption bands were seen with maxima at 300 and 650 nm (Fig. 1B). Under these irradiation conditions the products adsorbed on the surface presented emission and absorption bands in wavelength regions where Per also absorbs or emits. In contrast, at equal irradiation times no new emission bands (data not shown) were observed in those photolyzed in the presence of argon, although the diffuse reflectance spectra presented similar absorption bands. This suggests that the emitting adsorbed products result from the reactions of O_2 with adsorbed perylene as discussed below. A decrease in the photodegradation rate from 0.063 to 0.042 min^{-1} under an inert gas atmosphere ($r = 0.999$ and $r = 0.998$, respectively) was observed from the fluorescence intensity data as a function of irradiation time. These results [29] motivated the study herein presented on the effect of surface parameters, sample loading, and presence of coadsorbed species on the nature and yield of the principal products.

Because PAHs in atmospheric aerosols are found in a liquid-like environment [28], it was of interest to compare the photochemical behavior of Per in nonpolar and polar solvents to that adsorbed on the different surfaces. The irradiation of solutions of Per in different solvents resulted in the degradation of Per, based on the decrease on the intensity of the absorption and emission spectra as a function of the irradiation time (data not shown). Interestingly, formation of new bands at wavelengths above 450 and 550 nm in the absorption and emission spectra, respectively, were not observed. Bands in this region were observed for irradiated adsorbed samples. Only increases in the absorbance at wavelengths below 350 nm were detected in solution. This could imply a significant destruction of the extended π conjugated electronic system of Per.

Assuming a first order disappearance process, rate constants were calculated from plots of $\log(C/C_0)$ versus irradiation time. Values of k (h^{-1}) equal to 1.35, 0.73, 0.29, and 0.45 (correlation coefficient values between 0.996 and 0.999) were obtained for perylene dissolved in acetonitrile, methanol, hexane, and methanol/H_2O, respectively. These results indicate much faster rates in polar than in nonpolar solvents, and a quenching effect by water. These qualitative results suggested also a strong dependence of the photodegradation process mechanisms on the solvent polarity and on the surface effects exerted on the adsorbed molecule as demonstrated by the different nature of the products. In terms of the photochemistry of PAHs in the atmospheric particulate matter, these results demonstrated the value of photochemical studies of PAHs in the different controlled environments for understanding their transformation on the more complex matrix of the atmospheric particulate matter. The effect of solvent polarity on the photodegradation rates could be explained by the differences in the mechanisms of degradation reported by others which includes the participation of a perylene radical cation in polar solvents [31] or a solvent radical cation-Per anion pair in cyclohexane [32]. The results in polar solvents suggest that products resulting from the reactions of the Per radical cation can be expected.

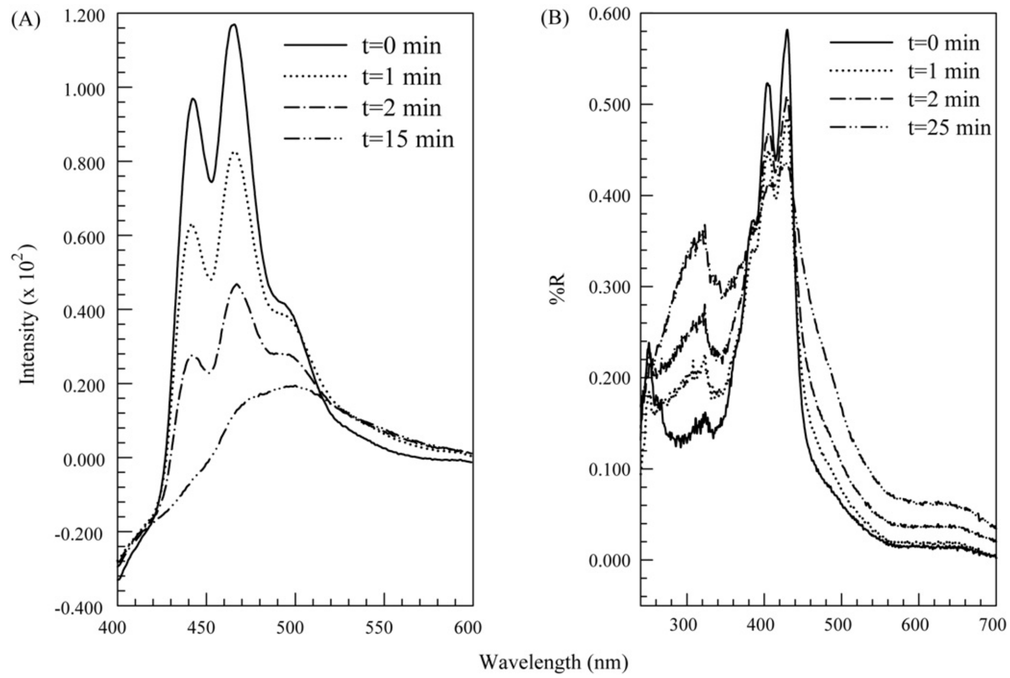

Fig. 1. (A) Emission, (B) diffuse reflectance spectra of perylene adsorbed on silica gel 60 Å at different irradiation times. Sample loading: 5×10^{-7} mol/g; excitation wavelength: 380 nm; oxygen atmosphere. excitation and emission slits set at 4 mm. Fluorescence measured at 45°.

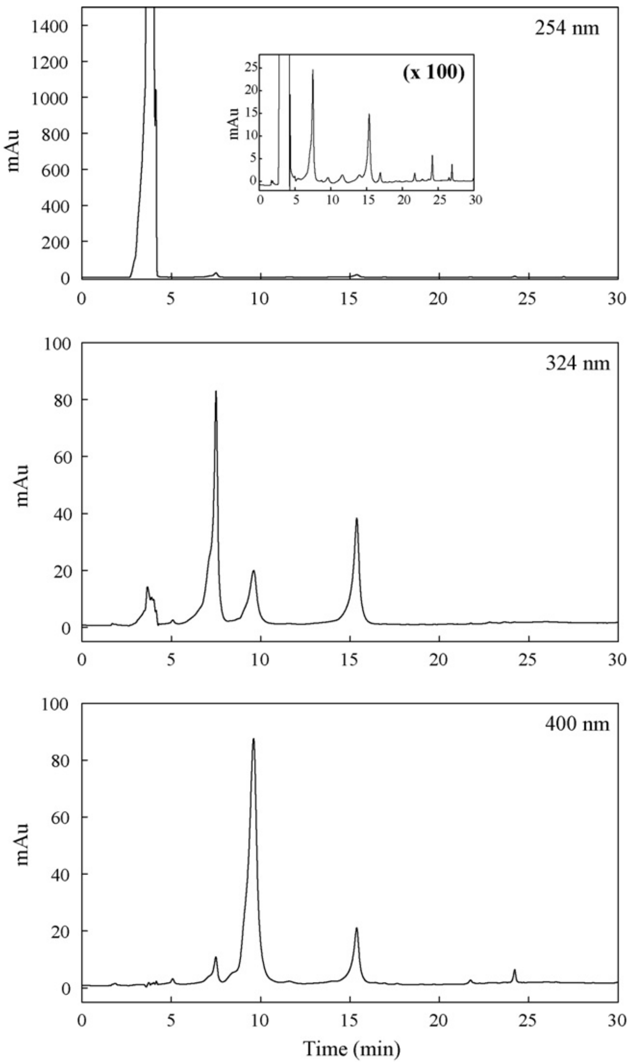

Fig. 2. HPLC Chromatograms of an extract of a sample of perylene adsorbed on silica gel 60 Å and irradiated for 30 min taken at 254, 324, and 400 nm. Mobil phase: acetonitrile/H_2O; flow rate: 1.00 mL/min.

3.2. Product properties and characterization

The characterization and identification of the stable photoproducts is of great relevance to their classification based on structure, reactivity, and toxicity, and to the elucidation of the mechanism of photodegradation of Per when adsorbed on surfaces. Three major products were observed in the chromatograms of extracts of irradiated samples (Fig. 2). These are identified according to their retention times ($R_t = 7$ min, $R_t = 9$ min and $R_t = 15$ min). On increasing the time of irradiation, other chromatographic peaks became evident in the chromatogram. As the major peaks decreased with irradiation time, five other peaks appeared ($R_t \approx 8$ min, $R_t \approx 11$ min, $R_t \approx 13$ min, $R_t \approx 20.4$ min, $R_t \approx 20.9$ min). Since the intensity of these was very small, it was difficult to integrate the peaks or to record their UV–vis spectra.

All the products had retention times shorter than Per ($R_t \approx 24.3$ min), suggesting a more polar character or fragmentation of the parent molecule. The larger polarity was due to the incorporation of oxygen functionalities to the aromatic system, as suggested by the appearance of absorption bands in the 450 nm region during the irradiation, the increase in the photodegradation rate in the presence of O_2 [29], and the product identification studies (discussed below).

The UV–vis absorption spectra and the photochemical kinetic curves for each of the major products are presented in Figs. 3–5. Compared to the absorption spectrum of Per, the absorption spectra of the products showed loss of the vibronic structure and the presence of another band with maximum between 450 and 460 nm, although the shape of the spectrum differed considerably among them. The fact that some of these products absorption bands appear in a wavelength region where Per also absorbs, could explain the observation that the product yields reached a plateau and then started to decrease with irradiation time due to their simultaneous photodestruction. The peaks at $R_t = 7$ min and $R_t = 9$ min were identified preliminarily as 1,12-perylenequinone and 3,10-perylenequinone, respectively, based on the absorption spectra reported by Nowakowska et al. [33]. The identity of 3,10-perylenequinone was corroborated by co-injection of a standard with the irradiated sample. Based on the shape of the UV–vis spectrum, which is similar to that of quinones of other PAHs for which the carbonyl functionalities are in opposite sides of the molecule, the chromatographic peak at $R_t = 15$ min (Fig. 5) could correspond to another quinone [34]. Other chromatographic peaks that were observed at longer irradiation times when the intensity of the principal products started to decrease ($R_t = 8$, 11, and 13 min), could be associated with quinones due to the proximity of their chromatographic peaks to those of the major products. The peaks with retention times at 20.4 and 20.9 min could correspond to hydroxyperylenes, and we suggest that these peaks are produced by secondary reactions. The formation rate of the products (Figs. 3–5) was also influenced by the surface. It was observed that the product with the largest percent yield (at the conditions used for their detection) in all the surfaces was the one at $R_t = 9$ min, identified as 3,10-perylenequinone. It was also the product that photodegraded faster, especially when adsorbed on silica gel 150 Å. On this surface the percent yield of the chromatographic peak with $R_t = 7$ min, preliminarily identified as 1,12-perylenequinone, was lower than on other surfaces. The percent yield of the product with $R_t = 15$ min was smaller in samples of Per adsorbed on alumina than in the other surfaces. Increasing the surface loading by a factor of ten resulted in a 50% decrease in the rates of both Per photodegradation and product formation. However, the relative product distribution yield remained the same, suggesting that none resulted from bimolecular reactions in the aggregates. In brief, these photochemical kinetic curves demonstrate that the rates of formation and yields of the products depend on the surface porosity, loading, and nature of the surface. In order to determine the percent of surface adsorbed Per transformed into the major products, an attempt was made to quantify the yield of each product. For a sample in which 94.6% of the Per was degraded, the number of moles of 3,10-perylenedione was calculated to be 1.51×10^{-9} (4.26×10^{-7} g). The response factors, f_ε, of the other products were not determined due to the unavailability of standards. Nonetheless, the molar absorption coefficient for the 1,12-perylenedione and for the product with retention time of 15 min were estimated by analyzing their respective absorption spectra (the band in the 400 nm wavelength region) and comparing it with that of the 3,10-perylenedione in the following manner. The ratios of the absorbance at 400 nm to the total band absorption (proportional to the integrated band absorption coefficient) for each compound were obtained and compared to that of 3,10-perylenedione. Then, each ratio was multiplied by the known absorption coefficient of the 3,10-dione to obtain the absorption coefficient of the unknown. From an analysis of the HPLC chromatogram recorded at $\lambda = 400$ nm, and by comparing the absorbance spectrum of the product at a particular wavelength, it was estimated that the molar absorption coefficient of

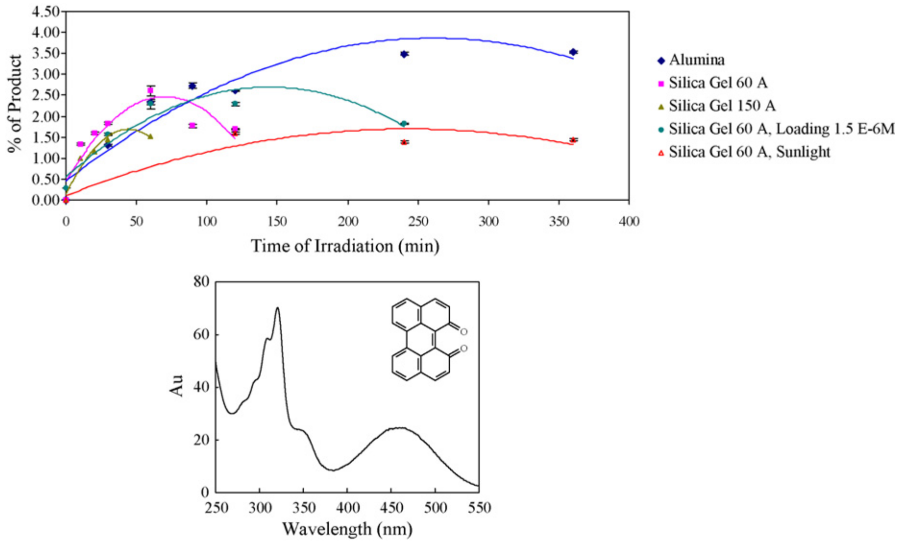

Fig. 3. Formation of 1,12-perylenedione on different surfaces as a function of irradiation time. Sample loading: 5×10^{-7} mol/g, unless otherwise specified; air atmosphere. These kinetic results were obtained by HPLC quantifications of the peak areas of the chromatograms. Percent yields are expressed in terms of percent starting material.

the 1,12-perylenedione and the other dione were, respectively, 1/8 and 1/4 of the value of the 3,10-perylenedione. The results shown in Table 1 demonstrate that at a 53.5% photodegradation of Per (4.4×10^{-9} mol of Per consumed), the yields of 3,10-perylenedione formed was twice as large as that for 1,12-perylenedione or the other dione. The total sum of the moles of products formed only accounted for close to 30% of the photodegradation of Per. This can be explained by (1) the photodegradation of products absorbing light in the same wavelength region as Per (Figs. 3–5), (2) the failure of other products to absorb at $\lambda < 300$ nm, (3) the lack of recovery of all products in the extraction procedure, although the diffuse reflectance and emission spectra of the extracted surfaces did not show evidence of residual absorptions or emission, and (4) possible thermal degradation during the extraction procedure.

Atmospheric Pressure Chemical Ionization (APcI) in the positive mode was used for further characterization of some of the products. The chromatographic peak at $R_t = 7$ min, preliminarily identified as 1,12-perylenequinone, gave a peak with an *m*/*z* value of 283 (Fig. 6) which corresponded to $(M+H)^+$ for a perylenequinone (formula: $C_{20}H_{10}O_2$; mass = 282 g/mol). The peak at $R_t = 9$ min identified as 3,10-perylenequinone also gave a peak with an *m*/*z* value of 283, which corroborated also its identity as a perylenequinone. In a similar fashion, the chromatographic peak at $R_t = 15$ min, suspected to be another perylenequinone, had an *m*/*z* value of 283, supporting its identity as another perylenequinone. The chromatographic peaks that eluted at $R_t = 20.4$ min and $R_t = 20.9$ min could be isomers, based on the proximity of the peaks and on the similarity of their UV–vis spectra. $APcI^+$ analysis of both chromatographic peaks resulted in parent ions with m/z of 285 (formula: $C_{20}H_{10}O_2$) which could correspond to $(M+H)^+$ for perylenediol (Fig. 7).

Using Daughter Ion Analysis (DAI), ions with *m*/*z* of 282 were allowed to pass through the collision cell where they

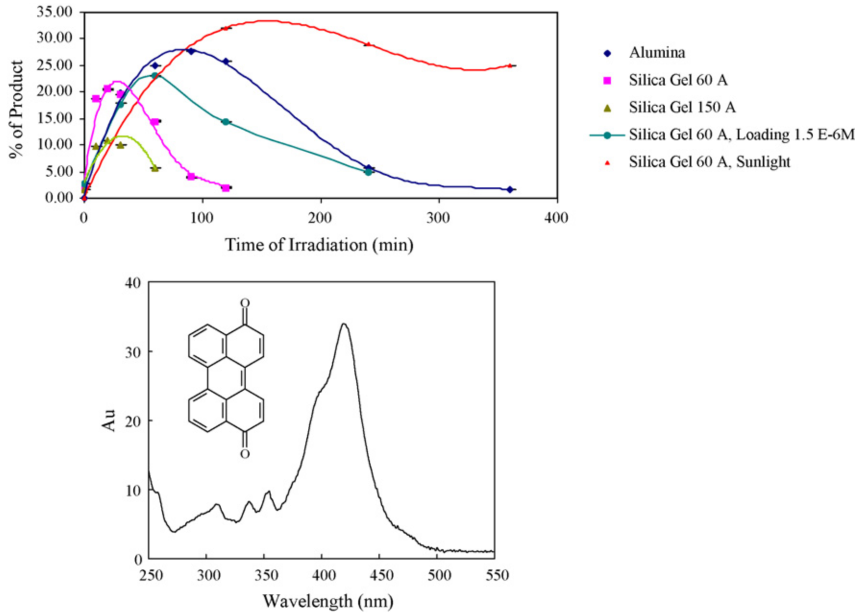

Fig. 4. Formation of 3,10-perylenedione on different surfaces as a function of irradiation time. Sample loading: 5×10^{-7} mol/g, unless otherwise specified; air atmosphere. These kinetic results were obtained by HPLC quantifications.

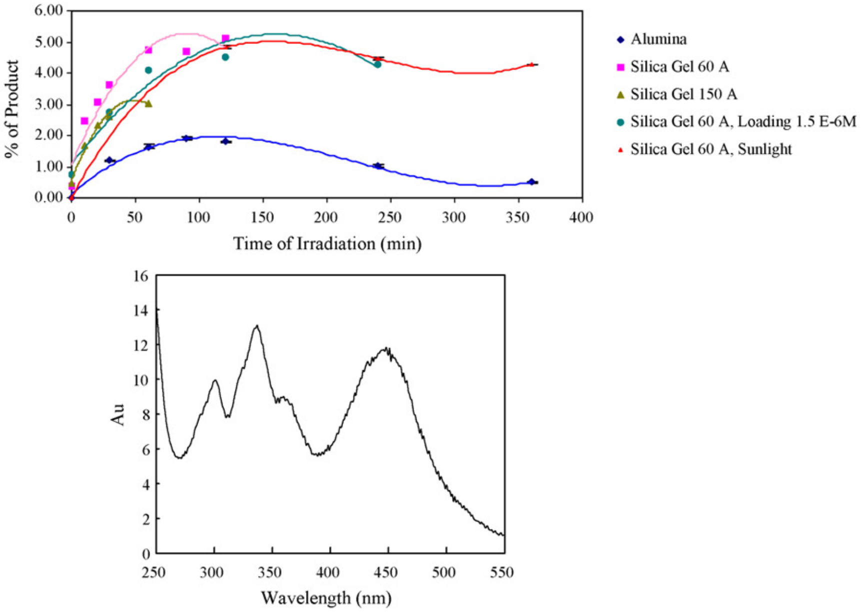

Fig. 5. Formation of the third major product ($R_t = 15$ min) on different surfaces as a function of irradiation time. Sample loading: 5×10^{-7} mol/g, unless otherwise specified; air atmosphere. These kinetic results were obtained by HPLC quantifications.

were bombarded and fragmented. For the three chromatographic peaks identified as perylenequinones ($R_t = 7$ min, $R_t = 9$ min, and $R_t = 15$ min) only three peaks with m/z values 225.8, 254.4 and 282 were observed, which corresponded to the quinone (data not shown). The appearance of only two fragments implied a large fragment stability of these molecules. The fragment with $m/z = 254$ could correspond to a loss of a C–O group (loss of mass = 28) while the other with a m/z of 225.8 (loss of mass = 56.2) could correspond to the loss of another C–O group. The similarity of the DAI spectra for the perylenequinones is evidence that their corresponding parent ions were similar, with the carbonyl groups located at opposite sides of the molecule. The fact that the chromatographic peak at $R_t = 7$ min (1,12-perylenequinone) exhibited a small peak at $m/z = 254$ suggested that it can be associated to an unstable product that losses both carbonyl groups simultaneously. This agreed with the results reported by Fatiadi et al. [35] in the sense that they found that 1,12-perylenequinone was very unstable, labile and tended to oxidize in air.

Table 1

Perylene + products in a sample of perylene adsorbed on silica gel 60 Å at different percent of photodegradation

Product/peak	Amount produced ($\times 10^{-9}$) moles		
	53.5%	74.3%	87.0%
1,12-Perylenedione	0.0 0.3*	0.1 0.4*	0.1 0.4*
3,10-Perylenedione	0.6	0.6	0.6
$R_t = 15$ min	0.1 0.3*	0.1 0.4*	0.1 0.4*
$R_t = 20.4$ min	0.060	0.02	0.04
$R_t = 20.9$ min	0.012	0.02	0.04
Perylene remaining on the surface[c]	3.8	2.1	1.1
Perylene (initial moles)[c]	8.2	8.2	8.2
Perylene (moles degraded)[c]	4.4	6.1	7.2
Moles of product formed[c]	0.7 1.2*	0.8 1.4*	0.8 1.5*
Percent yield[a] of products	16% 27%*	13% 23%*	23% 21%*
Total percent yield[b]	55% 61%*	35% 43%*	23% 32%*

* Corrected values (assuming that the value of the molar absorption coefficient was 8 times smaller for the product at $R_t = 7$ min and 4 times smaller for the product at $R_t = 15$ min).

[a] Percent yield = (moles of photoproducts/initial moles of perylene).

[b] Total percent yield = (moles of photoproducts + perylene remaining on the surface/initial moles of perylene).

[c] Calculated error = 0.3.

3.3. *Mechanisms of product formation: singlet oxygen, radical cation*

In an oxygen atmosphere the fluorescence emission of adsorbed perylene is quenched by about 70%, its photodegradation rate increases by 64% in comparison to samples irradiated under an inert gas atmosphere, and new changes in the absorption and emission bands are observed [29].

The direct photolysis of adsorbed Per on silica gel in the presence of air results in 100% degradation in a 1-h irradiation and the major products formed under these conditions are 3,10 and 1,12-perylene diones, another uncharacterized dione with retention time of 15 min, and five other products that include diols. These results suggest a strong participation oxygen reactive species in the photodegradation mechanism. To establish this participation several experiments, described below, were performed.

Irradiation of adsorbed Per on silica gel under low pressure conditions (to exclude some O_2) resulted in only 64% photodegradation after 4 h of photolysis as compared to 100% under an air atmosphere in a 1-h irradiation time. The chromatograms of the extracts presented 4 peaks of which three corresponded to the 1,12 and 3,10 perylenediones, the other dione ($R_t = 15$ min), and the fourth peak appeared at 16.5 min. This new product presented an absorption band with maximum at 405 nm and a shoulder at 380 nm. The spectrum is very similar to the spectrum of 3,10-perylenedione. Under these low pressure conditions the $^1O_2$ pathway nor the formation of a perylene radical cation through an electron transfer reaction of excited Per to O_2 should be present. Thus, the diones can be formed by the direct photoionization of Per to produce the radical cation which then reacts with adsorbed water (Scheme 1) that was not totally removed during the pumping process of 2 h at pressures less than 1 Torr. We have reported [29] that the tran-

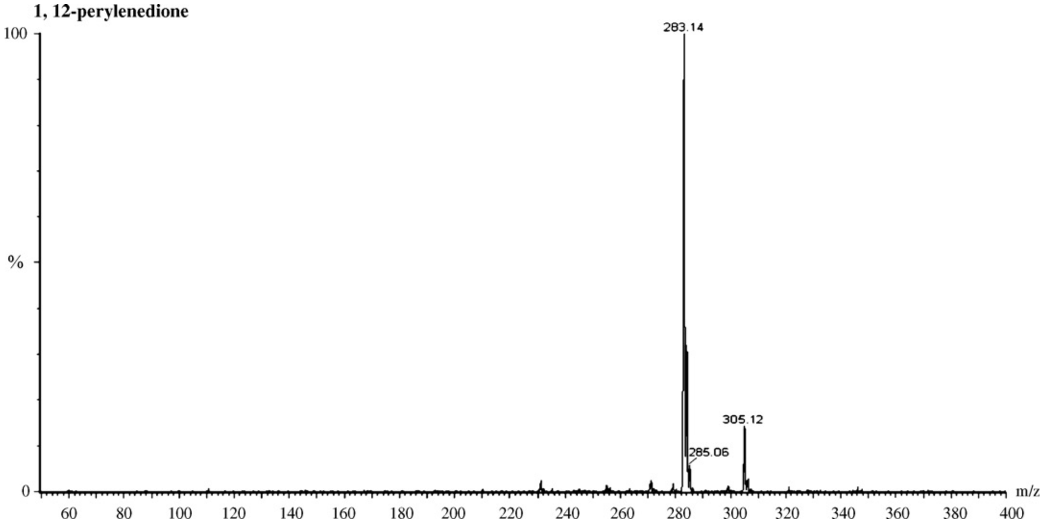

Fig. 6. APcI⁺ mass spectrum of 1,12-perylenedione (R_t = 7 min, mass = 282). Temperature of the source was 120° and temperature of the probe 600 °C. The cone and HV lens were set at 30 and 0.05 eV, respectively.

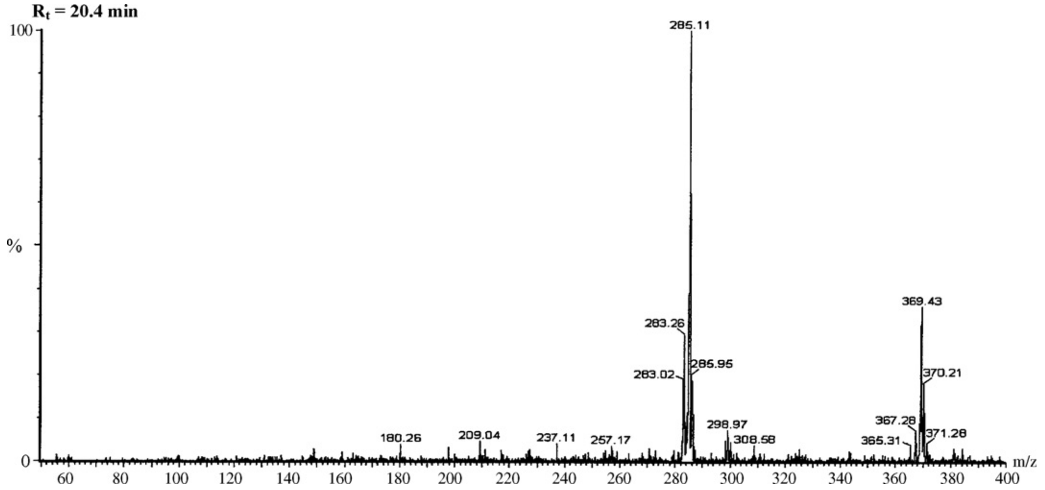

Fig. 7. APcI⁺ mass spectrum of the chromatographic peak with R_t = 20.4 min. Cone voltage: 30 eV. Temperature of the source was 120° and temperature of the probe 600 °C. The cone and HV lens were set at 30 and 0.05 eV, respectively.

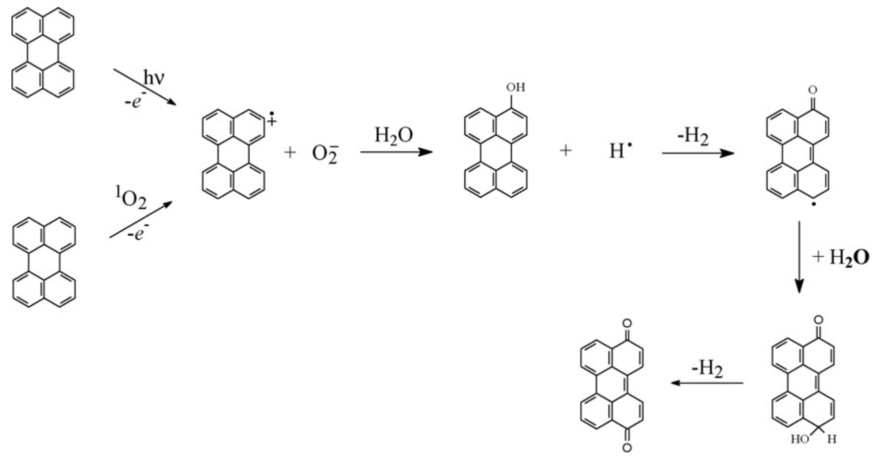

Scheme 1. Possible mechanism of formation of 3,10-perylenedione.

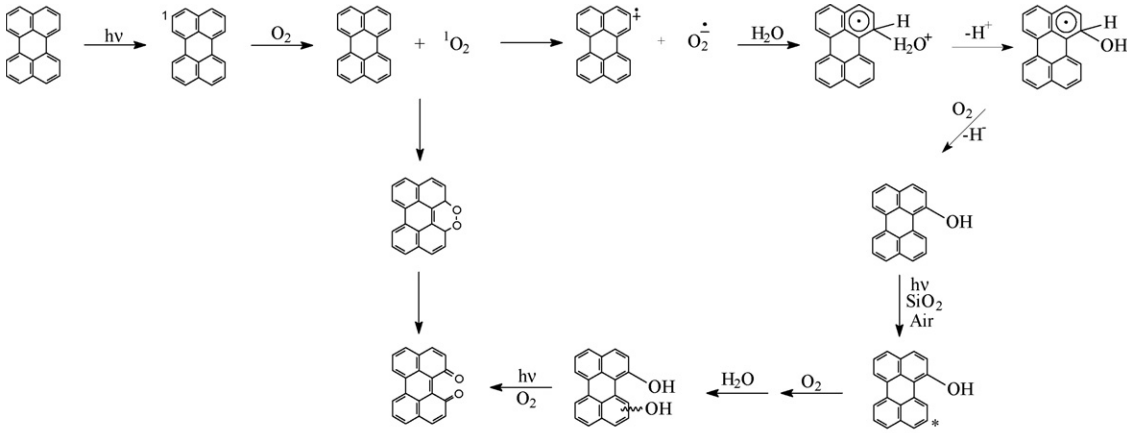

Scheme 2. Possible mechanism of formation of 1,12-perylenedione, adapted from Dabestani et al. [24].

sient diffuse reflectance spectrum of adsorbed Per irradiated with 266 or 355 nm laser pulses under a nitrogen atmosphere showed only the radical cation band with maximum at 540 nm and a small shoulder at 570 nm that suggest the presence of a radical anion. A triplet absorption band with maximum at 490 nm, seen in N_2(g) saturated acetonitrile solutions, was not observed on the adsorbed samples. The prompt appearance of the radical cation absorption signal within the nanosecond response time of the kinetic spectrometer strongly supports that the 266 or 355 nm laser pulse excitation induces the photoionization of adsorbed Per during subnanosecond time scale. Moreover, the ESR spectra of irradiated Per on silica gel at 77 K showed the previously reported spectrum of the Per radical cation.

In samples of perylene containing coadsorbed 2,5-dimethylfuran to trap singlet oxygen, the irradiation resulted in 96% degradation of the Per after 4 h of photolysis. For these samples, the chromatogram of the extracts showed only a very small yield of the diones suggesting the formation of $^1O_2$ through an energy transfer process from excited singlet Per and the rapid scavenging by DMF, thus quenching the formation of diones. Using Eq. (2) under the assumption that the rate constant for $^1O_2$ reaction with DMF is larger than with Per (k_q quenching of O_2 by DMF is $4 \times 10^8\,M^{-1}\,s^{-1}$, for Per has not been reported, but for anthracene $k_q = 10^5\,M^{-1}\,s^{-1}$ [36] and the experimental conditions surface loading DMF > Per), the percent of the products formed by the reaction of Per with $^1O_2$ and by the radical cation intermediate were obtained.

For the reaction with the $^1O_2$ the percentages were 72 for the formation of 1,12-perylenedione, 89 for the 3,10-perylenedione, and 57 for the uncharacterized dione ($R_t = 15$). Thus for the principal products, the $^1O_2$ pathway is predominant, although these could be produced through a radical intermediate species.

It has been reported that Per is one of the few PAHs that can produce $^1O_2$ by energy transfer process from either its excited singlet or triplet states [37–39]. Recently, a value of 0.28 for the efficacy of $^1O_2$ production by the excited singlet state of Per was reported while the value for other ten PAHs was zero [39]. Thus, in the case of adsorbed Per, where the intersystem crossing is smaller than in solution (0.009 methanol [40]), $^1O_2$ is formed by an energy transfer process from the excited singlet state of Per, which then reacts with a ground state Per to form the observed products. These can be formed through a Diels Alder cycloaddition reaction (1,12-perylenedione, Scheme 2) or through an electron transfer reaction from perylene to the singlet oxygen [41] and subsequent reactions of the perylene radical cation (3,10-perylenedione, Scheme 1). To confirm for the participation $^1O_2$ in the formation of the perylenediones, this species was produced by the excitation of methylene blue adsorbed on silica mixed with silica powder containing adsorbed perylene in the presence of air. After 14 h of irradiation, Per was degraded by 93% and the three main diones were detected in the extracts while the diols, observed in the direct photolysis, were not detected. The effectiveness of coadsorbed 2,5-dimethylfuran as $^1O_2$ scavenger was demonstrated in irradiated samples containing methylene blue as $^1O_2$ sensitizer, DMF, and perylene. In these, products were not observed.

The effect of surface pore size and of a different surface on the products percent yields (Figs. 3–5) can be then rationalized in terms of a decrease in the radical cation yield with an increase in the average pore diameter and on alumina [29]. Because 3,10-perylenedione is the product produced with the largest yield and its precursor is a radical cation, its lower yield in the larger pore size silica will have a larger effect in this dione than in the other products. Furthermore, we postulated [29] that in silicas of small pore diameters the closer proximity of $^1O_2$ to perylene would lead to a larger product yield in these surfaces.

It has been recently reported [42] that Per in dilute aqueous solution does not show evidence of photodegradation through a radical cation intermediate, in contrast to our results that show that adsorbed Per on silica gel photodegrades through a singlet oxygen and radical cation mediated combined mechanisms. These results demonstrate the importance of the surface-adsorbate interactions, and the differences in the photodegradation routes in the different environments found in the atmospheric aerosols.

Acknowledgements

We acknowledge the research financial support provided by the Minority Graduate Education Program, Compañía de Fomento Industrial de Puerto Rico and EPA-U.S.A., Grant R-8233-28-01, U.S. DOE/EPSCoR Grant DE-FG-02-94 ER-75764 and NIH-SCORE (Grant 5506GM08102). We also acknowledge Dr. Michael Sigman for the opportunity to work in his laboratory at Oak Ridge, Tennessee.

References

[1] R. Perry, R.M. Harrison, I.A. Davies, D. Ratnayaka, R.A. Wellings, Municipal incinerator as source of polynuclear aromatic hydrocarbons in environment, Environ. Sci. Technol. 10 (1976) 451–453.

[2] F.W. Karasek, G.A. Eiceman, R.E. Clement, Analysis of fly ash from municipal incinerators for trace organic compounds, Anal. Chem. 51 (1979) 2343–2350.

[3] R.M. Hoff, K. Chan, Measurement of polycyclic aromatic hydrocarbons in the air along the Niagara river, Environ. Sci. Technol. 21 (1987) 556–561.

[4] W. Lee, W. Chao, M. Shih, C. Tsai, T.J. Chen, P. Tsai, Emissions of polycyclic aromatic hydrocarbons from batch hot mix asphalt plants, Environ. Sci. Technol. 38 (2004) 5274–5280.

[5] S. Lundstedt, P. Haglund, L. Öberg, Simultaneous extraction and fractionation of polycyclic aromatic hydrocarbons and their oxygenated derivatives in soil using selective pressurized liquid extraction, Anal. Chem. 78 (2006) 2993–3000.

[6] B.D. Tebbens, J.F. Thomas, M. Mukai, Fate of arenes incorporated with airborne soot: effect of irradiation, Am. Ind. Hyg. Assoc. J. 32 (1971) 365–372.

[7] T. Novakov, S.G. Chang, Formation of pollution particulate nitrogen compounds by NO-soot and NH_3-soot gas-particle surface reactions, Atmos. Environ. 9 (1975) 495.

[8] K. Nikolaou, P. Masclet, G. Mouvier, Source and chemical reactivity of polynuclear aromatic hydrocarbons in the atmosphere—a critical review, Sci. Total Environ. 32 (1984) 103–132.

[9] R.G. Harvey, Polycyclic Aromatic Hydrocarbons, first Ed., Wiley-VCH, New York, 1997.

[10] B.J. Finlayson-Pitts, J.N. Pitts, Chemistry of the Upper and Lower Atmosphere: Theory, Experiments and Applications, Academic Press, San Diego, 2000.

[11] C. Arden Pope, R.T. Burnett, M.J. Thun, E.E. Calle, D. Krewski, K. Ito, G.D. Thurston, Lung cancer, cardiopulmonary mortality and long-term exposure to fine particulate air pollution, JAMA 287 (2002) 1132–1141.

[12] L.D. Hulett, A.J. Weinberger, K.J. Northcutt, M. Ferguson, Chemical species in fly ash from coal-burning power plants, Science 210 (1980) 1589–1616.

[13] R.A. Hites, T.D. Behymer, Photolysis of polycyclic aromatic hydrocarbons adsorbed on simulated atmospheric particulates, Environ. Sci. Technol. 19 (1985) 1004–1006.

[14] R.A. Hites, T.D. Behymer, Photolysis of aromatic hydrocarbons adsorbed on fly ash, Environ. Sci. Technol. 22 (1988) 1311–1319.

[15] G. Mamantov, T.D. Dunstan, E.L. Wehry, R.F. Mauldin, Z. Jinxian, A.D. Hipps, Adsorption and photodegradation of pyrene on magnetic, carbonaceous, and mineral subfractions of coal stack ash, Environ. Sci. Technol. 23 (1989) 303–308.

[16] M.E. Sigman, S.P. Zingg, Influence of SiO_2/cyclohexane interface on the photochemistry of anthracene, Photochem. Photobiol. 57 (1993) 453–459.

[17] M.E. Sigman, J.T. Barbas, E.A. Chevis, R. Dabestani, Spectroscopy and photochemistry of 1-methoxynaphthalene on SiO_2, New J. Chem. 20 (1996) 243–248.

[18] M.E. Sigman, J.T. Barbas, R. Dabestani, Photochemical oxidation of phenanthrene sorbed on silica gel, Environ. Sci. Technol. 30 (1996) 1776–1780.

[19] M.E. Sigman, J.T. Barbas, R. Arce, R. Dabestani, Spectroscopy and photochemistry of fluorene at a silica gel/air interface, J. Photochem. Photobiol. A: Chem. 109 (1997) 229–236.

[20] M.E. Sigman, R. Arce, C.A. Reyes, J.T. Barbas, R. Dabestani, Photochemistry of acenaphthene at a silica gel/air interface, J. Photochem. Photobiol. A: Chem. 112 (1998) 277–283.

[21] R. Dabestani, J.T. Barbas, M.E. Sigman, A mechanistic study of photodecomposition of acenaphthylene on a dry silica surface, J. Photochem. Photobiol. A: Chem. 80 (1994) 103–111.

[22] R. Dabestani, K.J. Ellis, M.E. Sigman, Photodecomposition of anthracene on dry surfaces: products and mechanism, J. Photochem. Photobiol. A: Chem. 86 (1995) 231–239.

[23] R. Dabestani, M.E. Sigman, M. Nelson, Photochemistry of tetracene adsorbed on dry silica: products and mechanism, Photochem. Photobiol. 64 (1996) 80–86.

[24] R. Dabestani, C.A. Reyes, M. Medina, C.E. Crespo-Hernández, M.Z. Cedeño, R. Arce, O. Rosario, D.M. Steffenson, I.N. Ivanov, M.E. Sigman, Photochemistry of pyrene on unactivated and activated silica surfaces, Environ. Sci. Technol. 34 (2000) 415–421.

[25] J.T. Barbas, M.E. Sigman, A.C. Buchanan, E.A. Chevis, Photolysis of substituted naphthalenes on SiO_2 and Al_2O_3, Photochem. Photobiol. 58 (1993) 155–158.

[26] R. Arce, S. Fioressi, Excited states and intermediate species of Benzo[e]pyrene photolyzed in solution and adsorbed on surfaces, J. Phys. Chem.: A 107 (31) (2003) 5968–5975.

[27] R. Arce, S. Fioressi, Photochemical transformations of Benzo[e]pyrene in solution and adsorbed on silica and alumina surfaces, Environ. Sci. Technol. 39 (2005) 3646–3655.

[28] S.R. McDow, Q-r. Sun, M. Vartiainen, Y. Hong, Y. Yao, T. Fister, R. Yao, R.M. Kamens, Effect of composition and state of organic components on polycyclic aromatic hydrocarbon decay in atmospheric aerosols, Environ. Sci. Technol. 28 (1994) 2147–2153.

[29] R. Arce, P. Sotero, Surface adsorbates effects on the photochemistry and photophysics of adsorbed perylene on unactivated silica gel and alumina, J. Photochem. Photobiol A: Chem. 167 (2004) 191–199.

[30] D.F.S. Natuseh, W.A. Korfmaker, E.L. Wehry, G. Mamantov, Resistence to photochemical decomposition of polycyclic aromatic hydrocarbons vapor-adsorbed on coal fly ash, Environ. Sci. Technol. 14 (1980) 1094–1099.

[31] R. Konuc, J. Cornelisse, S.P. McGlynn, Photoionization of perylene in polar solvents, J. Chem. Phys. 82 (1985) 3929–3933.

[32] M. Lamotte, J. Pereyre, J. Joussot-Dubrón, R. Lapouyade, The photolysis of pyrene and perylene in cyclohexane liquid solution from highly excited electronic states, J. Photochem. 38 (1987) 177–188.

[33] M. Nowakowska, J.E. Guillet, B. White, Studies of the antenna effect in polymer molecules: photosensitized oxidation of perylene in an aqueous solution of poly(sodium styrenesulfonate-*co*-2-vinylnaphthalene), J. Photochem. Photobiol A: Chem. 50 (1989) 147–156.

[34] A. Bjorseth (Ed.), Handbook of Analytical and Spectral Data for PAH, vol. I, Midwest Research Institute, Kansas City, Missouri, 1993.

[35] A.J. Fatiadi, Preparation and purification of some oxidation products of perylene, J. Res. Natl. Bureau Stds.–A. Phys. Chem. 72A (1968) 39–47.

[36] N.J. Turro, Modern Molecular Photochemistry, Benjamin Cummings, California, 1978.

[37] A.M. Trozzolo, K.C. Wu, Production of singlet molecular oxygen from the oxygen quenching of the lowest excited singlet state of aromatic molecules in n-hexane solution, J. Phys. Chem. 83 (1979) 3180–3183.

[38] T.J. Truscott, A.J. McLean, D.L. McGarvey, C.R. Lambert, E.J. Land, Effect of oxygen-enhanced intersystem crossing in the observed efficiency of formation of singlet oxygen, J. Chem. Soc. Faraday Trans. 86 (1990) 3075–3080.

[39] F. Wilkinson, D.R. Worrall, A.A. Abdel-Shafi, Singlet oxygen formation efficiencies following quenching of excited singlet and triplet states of aromatic hydrocarbons by molecular oxygen, J. Photochem. Photobiol. A: Chem. 142 (2001) 133–143.

[40] C.A. Parker, T.A. Joyce, Formation efficiency and energy of the perylene triplet, Chem. Commun. 4 (1966) 108–109.

[41] D.R. Kearns, Physical and chemical properties of singlet molecular oxygen, Chem. Rev. 71 (1971) 395–427.

[42] N.V. Blough, M.P. Fasnacht, Mechanisms of the aqueous photodegradation of polycyclic aromatic hydrocarbons, Environ. Sci. Technol. 37 (2003) 5767–5772.